Removal of Malachite Green Dye from Waste Water Using Rice Husk Ash as an Adsorbent

Peram Shyamsundar Reddy[1], D Prasanna Kumar Reddy[2], Shaik Waqar[3],
K Naveen[4], Prof T Bala Narasiah[5]

[1][2][3][4][5] *Department of Chemical Engineering, JNTUA College of Engineering, Ananthapur, Andhra Pradesh,
India.*
Corresponding Author: Peram Shyamsundar Reddy

---ABSTRACT--

In the current study, the feasibility of using Rice Husk Ash (RHA) to remove Malachite Green Dye (MG) from wastewater has been explored as a low cost and eco-friendly adsorbent. Effecting factors like adsorbate concentrations by varying the amount of adsorbent, temperature, pH, initial concentrations, contact time and agitation speeds on the adsorption of malachite green were examined using batch experiments. With the aid of UV-Spectrophotometer, the concentration of MG was calculated for before and after adsorption. Characterization of RHA was done with advanced techniques like DLS, XRD, FTIR and SEM/EDS. Thermodynamics parameters like ΔH°, ΔS° and ΔG° were estimated. Adsorption isotherms and adsorption kinetics were plotted and the best suitable fitting models were advised.
KEYWORDS; - *Rice Husk Ash, Malachite Green, Adsorption, Characterization, Thermodynamics, Kinetics, Isotherms.*

I. INTRODUCTION

A dye can be illuminated as 'A colored material which has affinity to the substrate to which it is being applied'. It can be used as an aqueous solution in textile industries and required a mordent for the improvement of fastness of dye on the fiber. Wastewater effluents from textile industries containing dyes causes a hidden hazard to the environment. The disposal of wastewater containing dyes without proper treatment is a big threat. Hence, these dyes are to be evacuated from the water bodies. Different dye removal approaches are divided into chemical, physical and biological methods. Physical methods are adsorption, ion exchange and filtration methods etc.., whereas chemical methods are ionization, photo catalytic reactions and Fenton Reagent etc.., and biological methods are aerobic / anaerobic degradation and bio-sorption etc.., Amongst stated, adsorption process is the most effective and cheap process with non-conventional adsorbents.. Hence, experimental studies in search of efficient and low cost adsorbents are gaining more importance to remove dyes from wastewater.

Rice husk is generated in Rice Mills during milling of paddy. It has granular structure, insoluble in water and has good chemical stability and mechanical strength. During firing process, the husk will be converted into ash, which is called as Rice Husk Ash (RHA). It contains around 85-90% of amorphous silica and is a cheaply available assert for various applications. Generally, around 12% of synthetic dyes were lost during processing and manufacturing operations, and 20% of resultant color enter into the environment over industrial wastewater effluents. Like other dyes, Malachite green (MG) is widely used as a synthetic and cationic dye in paper & pulp, leather and textile industries with molecular formula of $C_{23}N_2H_{25}Cl$. MG is a strong acid with moderate toxicity and extreme irritant in nature.

The current study was done to check out the feasibility of establishing an effective method to remove MG dye from wastewater using RHA as an adsorbent.

II. MATERIALS and METHODS

2.1 Preparation of adsorbent:

Rice Husk Ash, an agricultural waste product which is rich in silica about 85% - 90%. A known quantity of rice husk was burnt for 3 hours in a hot air oven at 110°C. The obtained ash was collected and sieved through BS standard sieves. Dynamic Light Scattering (DLS) was used to determine the average particle size of RHA.

2.2 Preparation of stock solution:
        One gram of commercially available Malachite Green Dye was taken and dissolved in one liter of distilled water in order to prepare a stock solution of 1000 mg/L. Experimental MG dye solutions of varying concentrations were prepared by series of dilution of stock solution with required volume of distilled water.

2.3 Plotting of calibration curve:
        Required quantity of MG dye was taken and measured with the help of electronic weighing balance, then mixed with suitable amount of distilled water to make sample solutions with varying dye concentrations. The % absorbance values were determined with the help of UV-Spectrophotometer at a wavelength (λ_{max}) of 540 nm. Using the equation of curve to find the concentrations at different % absorbance values, a calibration cure was plotted as shown in Fig.3.

2.4 Batch adsorption studies:
        Batch adsorption experiments were done to investigate the adsorption of MG dye on RHA. The effecting factors like initial concentration of MG dye, contact time, adsorbent dosage, pH, RPM and temperature were examined. At regular intervals of time, the adsorbent was filtered and the residual concentrations were analyzed with UV-Spectrophotometer at a wavelength of 540 nm until the equilibrium was reached. The amount of adsorption experimentally, q_e (mg/g) was given by

$$q_e = (C_o - C_e) / W * V \qquad (1)$$
$$\text{Removal (\%)} = (C_o - C_e)/C_o * 100 \qquad (2)$$

Where C_o and C_e (mg/L) are liquid phase concentrations of MG at initial and at equilibrium respectively, V is the volume of the solution in Liters and W is the mass of RHA adsorbent used in grams.

2.5 Adsorption Thermodynamics:
  Thermodynamic parameters like change in Gibbs free energy (ΔG_0), Enthalpy (ΔH_0) and Entropy (ΔS_0) were calculated through the equations given below

$$\Delta G_0 = -RT * \ln K_D \qquad (3)$$
$$K_D = q_e / C_e \qquad (4)$$
$$\ln K_D = (\Delta S_0 / R) - (\Delta H_0 / RT) \qquad (5)$$

Where K_D is the adsorption equilibrium constant, ΔG_0 was given from the classical Van't Hoff' equation, ΔH_0 and ΔS_0 were calculated from the slope of ln K_D against 1/T.R is the universal gas constant (8.314 J/mole) and T is the adsorption temperature (K).

2.6 Adsorption Kinetics:
The pseudo-first order rate equation is as follows

$$\ln (q_e - q_t) = \ln q_e - k_1 t \qquad (6)$$

The pseudo-second order rate equation is as follows

$$t/q_t = (1 / k_2 q_e^2 + t / q_e) \qquad (7)$$

Where k_1 and k_2 are the pseudo –first order rate constant and pseudo-second order rate constant, respectively. q_e and q_t are the adsorbent's adsorption capacity at equilibrium and at time t, respectively

2.7 Adsorption Isotherms:
2.7.1 Freundlich Adsorption Isotherm:
It is based on the assumption that adoption takes place on a heterogeneous surface. The isotherm equation is as follows

$$\ln q_e = \ln K_f + 1/n * \ln C_e \qquad (8)$$

2.7.2 Langmuir Adsorption Isotherm:
        It is based on the assumption that there are no interactive forces between the adsorbate molecules and the process is centralized in a monolayer on the fact that there is no interaction between the adsorbate molecules and the adsorption process is localized in a monolayer. When a dye molecule is occupied on a particular site, then there will be no further adsorption will take place at that particular site. The isotherm equation is as follows

$$\frac{C_e}{q_e} = \frac{1}{q_{max} K_L} + \frac{C_e}{q_{max}} \qquad (9)$$

III. RESULTS AND DISCUSSION
3.1 Characterization:
3.1. 1 Sieve Analysis:
A known quantity of Rice Husk Ash (RHA) was crushed in a crucible and sieved against the meshes ranging from 0, 60, 85,100 and pan. Required particle size of RHA with mesh > 85 and <100 mesh range was preferred and the results of sieve analysis was shown in Table 3.1

S.No	Mesh range	Diameter	Average Diameter D_{pi}	Weight Retained	Mass Fraction X_i	X_i/D_{pi}	X_i/D_{pi}^2	X_i/D_{pi}^3	X_i*D_{pi}
1	0	0	0	0	0	0	0	0	0
2	60	0.251	0.1255	9	0.03	0.239	1.9044	15.1745	0.003765
3	85	0.177	0.214	62.5	0.2083	0.973	4.5467	21.2463	0.0445
4	100	0.151	0.164	147.5	0.4916	2.997	18.274	111.4268	0.0806
5	Pan	0	0.0755	81	0.27	3.576	47.364	627.3377	0.020385
			Total	300	0.9999	7.785	72.0891	775.1853	0.14925

Table 3.1 Sieve analysis of RHA

From the Table 3.1,
Average particle size D_s = $1 / \Sigma (X_i/D_{pi})$ = 0.12845 mm
Mass mean diameter D_w = $\Sigma (X_i*D_{pi})$ = 0.14925 mm
Volume mean diameter D_v = $(1 / \Sigma (X_i/D_{pi}^3))^3$ = 0.10886 mm

3.1.2 FTIR Analysis:
Fourier Transform Infra-Red Spectroscopy (FTIR) is used to study molecular structure, identify the adsorbed species or reaction intermediates and their structures. From Figure 3.1 & 3.2, the FTIR studies for RHA was done with a scanning range of 4000 - 500 cm^{-1}. The broad peak at 3429.59 - 4000 cm^{-1}stretch was indicated the existence of -OH & -NH functional groups. The peaks observed at 2923.40 and 1383.59 cm^{-1} were due to stretching and bending C-H bond in methyl groups respectively. The peak at 2852.72 cm^{-1} was due to characteristic vibrations of –OH from carboxylic acids. The peaks observed between 1597.60 – 1744.68 cm^{-1} were due to presence of carbonyl groups. Due to −OH group alongside carbonyl group, indicated the presence of carboxylic groups in the rice husks. The peak at 1597.60 cm^{-1} was due to the presence of aromatic groups whereas the strong peak at 1094.44 cm^{-1} was due to C-O bending. The −OH, −NH, carbonyl and carboxyl groups were vital sorption sites. Some peaks were shifted after adsorption (3429.59 to 3433.36 cm$^{-1,}$ 2923.40 to 2923.56 cm^{-1}, 2852.72 to 2853.05 cm^{-1}, 1744.68 to 1745.18 cm$^{-1,}$ 1597.60 to 1617.07 cm$^{-1,}$ 1383.59 to 1383.29 cm$^{-1,}$ 1094.44 to 1095.63 cm^{-1} and 793.79 to 793.61 cm$^{-1)}$ whereas other peaks were appeared after adsorption (3851.15 cm^{-1}, 2351.39 cm^{-1} and 1457.24 cm^{-1}). From the FTIR analysis, this was a clear indication that adsorption of MG onto RHA had been taken place and new bonds were formed between MG and RHA.
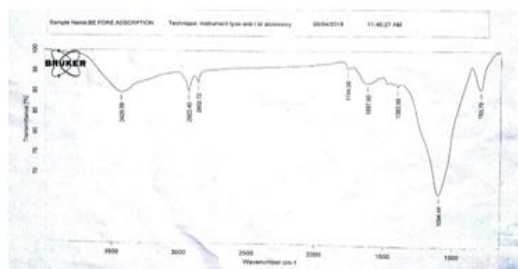

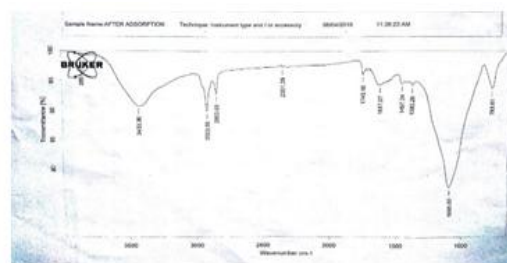**Fig.3.1.** FTIR spectrum of RHA before adsorption   **Fig.3.2**. FTIR spectrum of RHA after adsorption

3.1.3 Particle Size Analysis by DLS:
The Dynamic Light Scattering technique (DLS) which measures the hydrodynamic radius was used to produce the average size distribution as shown in Figure 3.3. The average particle size of rice husk ash was obtained from DLS technique is 284.2 nm.
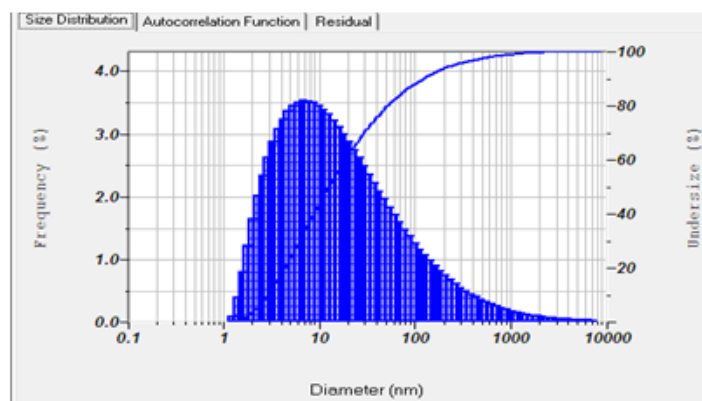
Fig.3.3.DLS analysis of RHA

3.1.4   X-Ray Diffraction:

X-ray diffraction (XRD) is an effective method for determining the crystal structure of materials, which can detect crystalline materials having domains greater than 3-5 nm. It is also used for characterization of crystal structure and chemical phase composition. The average crystal size of RHA can be determined by Scherer formula using X-Ray Diffractometer

$$X_s = 0.9 \, \lambda \, / \, (fwhm \, Cos \, \alpha) \qquad (10)$$

Where X_s is the crystallite size (nm), λ is the wavelength of the monochromatic X-ray beam (nm), fwhm is the ''full width at half-maximum'' for the diffraction peak under consideration (rad), and α is the diffraction angle (degree). From the analysis, RHA was found to be an amorphous and contains a heterogeneous surface as shown in Fig.3.4.
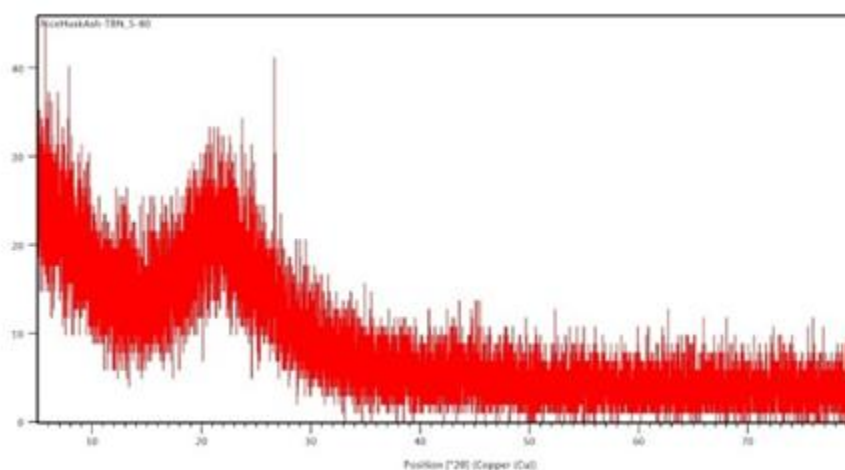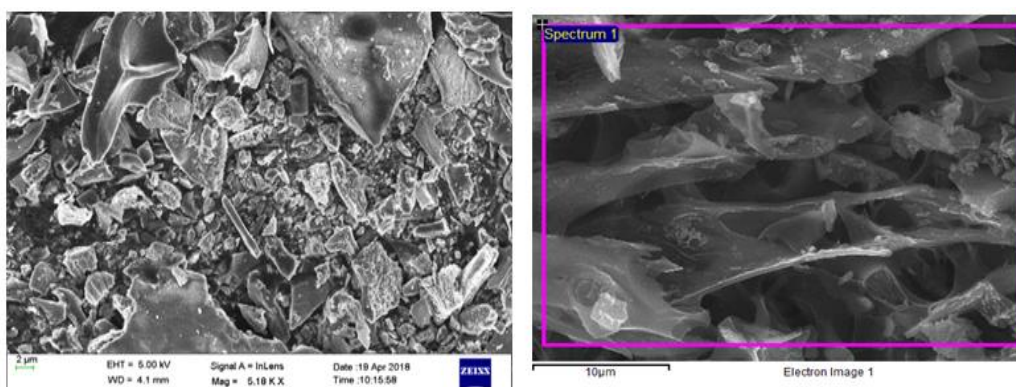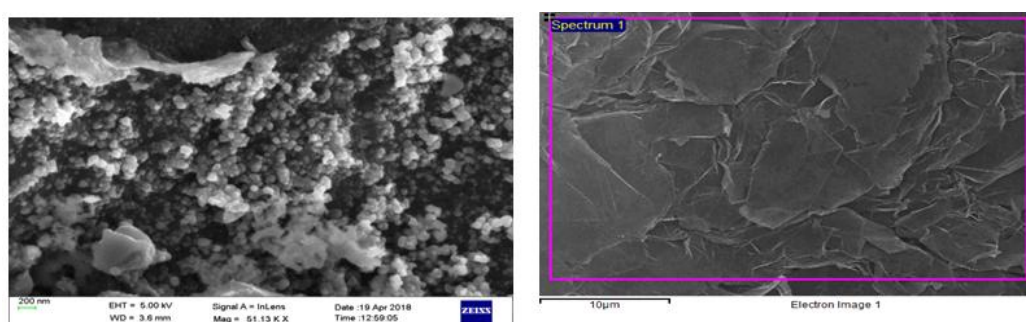

Fig.3.4.XRD analysis of RHA

3.1.5 SEM / EDS Analysis:

Scanning Electron Microscopy (SEM) is used to study the microscopic structure with an image magnification from about 20x to greater than 100,000x. It is also used to determine the physical properties like porosity, particle shape of adsorbent materials. From the SEM surface morphology analysis of RHA as shown in Fig 3.5 & 3.6, it was found that there were holes and cave type openings on the surface of the adsorbent which would have more surface area available for adsorption. However, following dye adsorption the particle surface become much smoother than that of the original particle. It was proven that the surface morphologies of RHA before and after adsorption were quite different.

(a)   (b)

Fig. 3.5. SEM images (a & b) of RHA before adsorption


(c)   (d)

Fig. 3.6. SEM images (c & d) of RHA after adsorption

Energy Dispersive X-Ray Spectroscopy (EDS) is used to determine elemental analysis. Typical EDS analysis of RHA, obtained from SEM was shown in Fig.3.7 & 3.8 showing the sample region probed and the spectra was obtained for RHA before and after adsorption respectively. It was observed that the domination of silicon and oxygen from the silica. The EDS chemical analysis values for RHA before and after adsorption was given in Table 3.2.
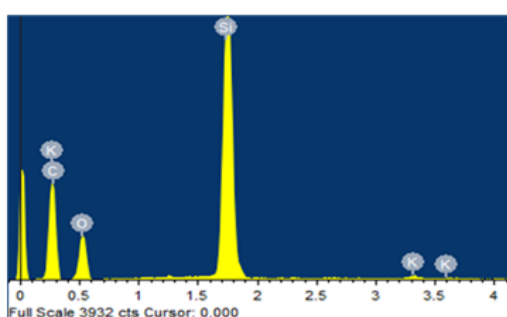
Fig. 3.7. EDS analysis of RHA before adsorption
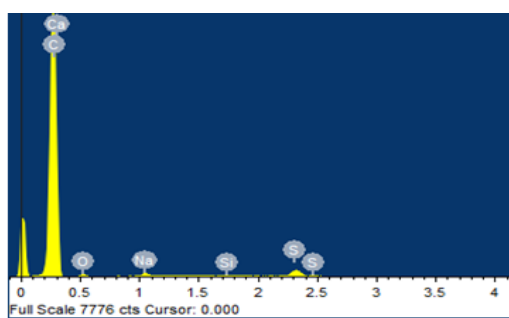
Fig. 3.8 EDS analysis of RHA after adsorption

Element	EDS analysis of RHA before adsorption		EDS analysis of RHA after adsorption	
	Weight%	Atomic%	Weight%	Atomic%
C K	93.84	95.89	90.27	93.62
O K	4.36	3.35	5.97	4.65
Na K	0.52	0.28	1.83	0.99
Si K	0.13	0.05		
S K	1.05	0.40	1.75	0.68
Ca K			0.18	0.06
Totals	100.00		100.00	

Table 3.2 EDS analysis of RHA before and after adsorption
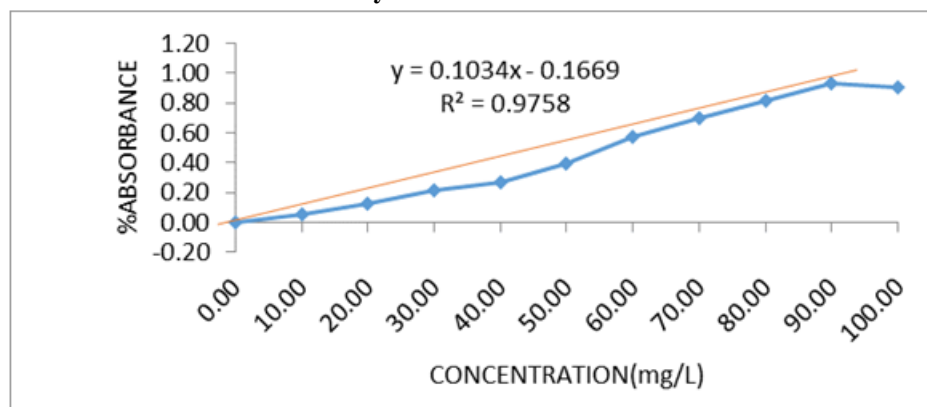
3.2 Calibration Curve of Malachite Green Dye

Fig.3.9. Calibration curve of Malachite Green Dye

3.3 Adsorption Studies
3.3.1 Effect of contact time:
The effect of contact time on adsorption of MG was examined with 10 mg/L initial dye concentration and an adsorbent dosage of 0.1g and keeping all other parameters as constant (T = 30^0C, RPM = 100, V=200 ml) with the help of orbital shaker. In the initial stage, the rate of adsorption was too fast due to adsorption of dye molecule onto the exterior surface**.** The Fig.3.10 indicated that the efficiency of dye adsorbed was rapid in initial stage up to 30 min and later it was slowed. The equilibrium was attained at 100 min and remains almost constant due to saturation of active site and no further adsorption will take place.
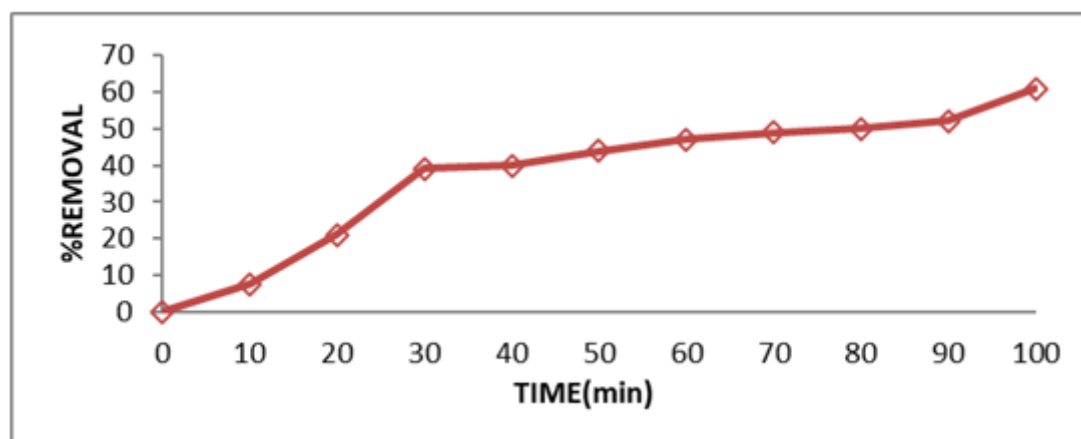

Fig.3.10. Effect of contact time on %Removal of MG

3.3.2 Effect of initial dye concentration:
The effect of initial dye concentration on adsorption of MG was examined as a function of contact time with 10 mg/L, 8 mg/L and 6 mg/L initial dye concentrations with an adsorbent dosage of 0.1g and keeping all other parameters as constant (T = 30^0C, RPM = 100, V=200 ml). It was observed that from Fig.3.11, after the formation of monolayer at the lower initial concentration of dye over the adsorbent surface and if any further formation of layer of dye species is highly hindered. It was observed that with increase in initial dye concentration, the adsorption capacity also increases providing a powerful driving force to overcome the mass transfer resistance between the aqueous and solid phases.
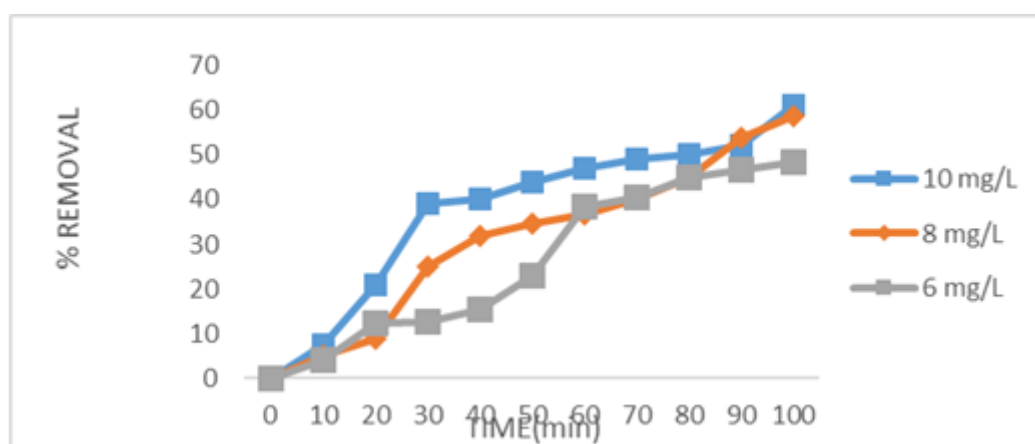
Fig.**3.11.** Effect of initial dye concentration on %Removal of MG

3.3.3 Effect of adsorbent dosage:

The effect of adsorbent dosage on adsorption of MG was examined as a function of contact time with constant 10 mg/L initial dye concentrations by varying the adsorbent dosage 0.05g, 0.1g and 0.15g and keeping all other parameters as constant (T = 30^0C, RPM = 100, V=200 ml) with the help of orbital shaker. It was observed in Fig.3.12 as the adsorbent dosage increases, the MG dye removal also increases, which can attribute to increase MG surface area and the availability of more active adsorption sites. When the equilibrium was attained, there was a decrease in amount of adsorption due to aggregation of adsorption sites which results in decreasing the total adsorbent surface area available for MG to be adsorbed.
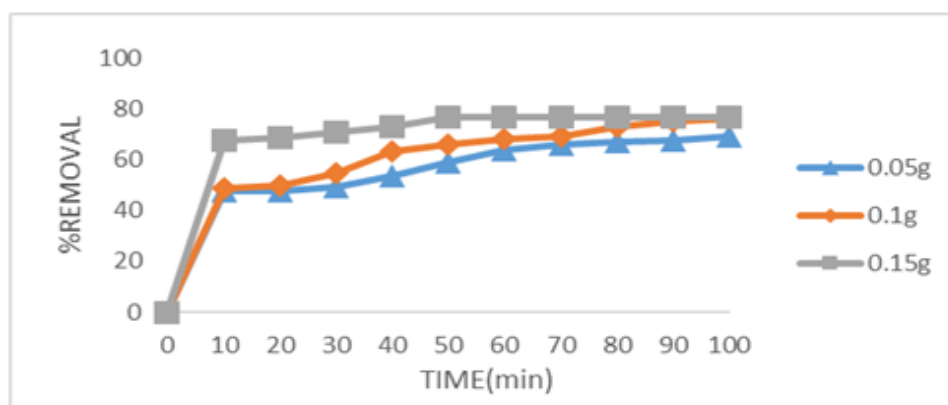

Fig.3.12. Effect of adsorbent dosage on %Removal of MG

3.3.4 Effect of agitation speed / RPM:

The effect of agitation speed or revolutions per minute (RPM) on adsorption of MG was examined as a function of contact time by using a range of shaking speeds (50-150 RPM) with 10 mg/L initial dye concentration and an adsorbent dosage of 0.1g and keeping all other parameters as constant (T = 30^0C, V=200 ml) with the help of orbital shaker. It was observed that as the RPM increases, the amount of adsorption is increased. Thus, agitation speed showed marked effect on the up take of dye at lower speeds. However, on further increase in agitation speed the uptake of dye is not much effected on the equilibrium time remains unaltered as observed in Fig.3.13. It was observed that with increase in the agitation speed, decreases the boundary of transfer of dye molecules from the bulk solution to adsorbent surface.
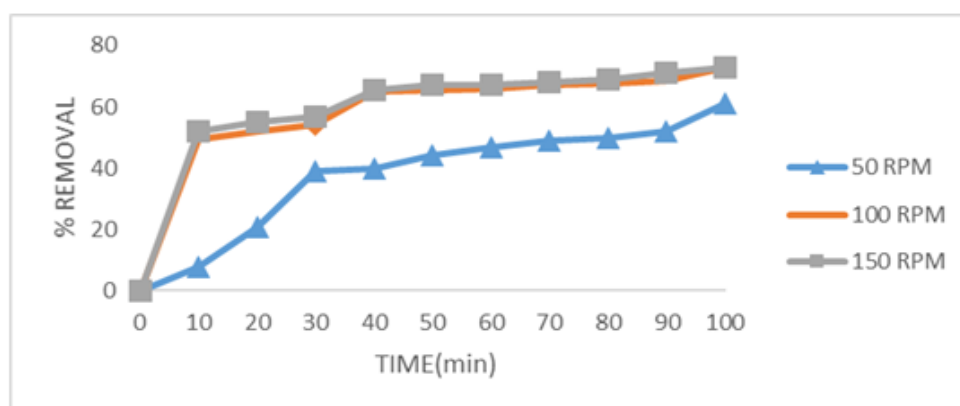
Fig. 3.13. Effect of agitation speed on %Removal of MG

3.3.5 Effect of pH:

The effect of pH of the solution on adsorption of MG was examined with 10 mg/L initial dye concentration and an adsorbent dosage of 0.1g by keeping all other parameters as constant (T = 30^0C, RPM = 100, V=200 ml) with the help of orbital shaker. The pH of dye solutions being 4, 6, and 8 were made and adjusted with dilute HCl (0.1 N) or KOH (0.1 N) solution by using a pH strips. From Fig.3.14, the maximum color removal was observed at pH = 8 and there was no significant in color removal after pH =8. It was observed that increase in dye adsorption depends on the properties of the adsorbent surface and the dye structure. MG will become protonated in the acidic medium, deprotonating takes place at higher pH consequently the positive charge density would be more on dye molecules at low pH, and results for higher up take on the negatively charged surface for adsorbent.
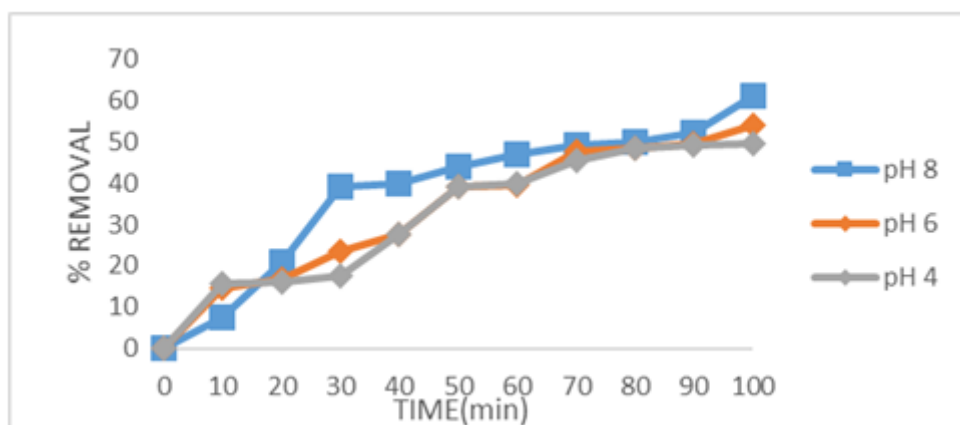

Fig.3.14. Effect of pH on %Removal of MG

3.3.6 Effect of temperature:

The effect of temperature on adsorption of MG was examined as a function of contact time with 10 mg/L initial dye concentration and an adsorbent dosage of 0.1g carried out at temperature range of 30^0C to 50^0C with the help of orbital shaker (RPM=100, V=200ml). From Fig.3.15, it was observed that an endothermic process because of dye increased surface activity and kinetic energy of solute molecules controlled the adsorption of dye increases with increasing temperatures and the dye adsorption process. Thermodynamic parameters like changes in Gibbs free energy (ΔG˚), Enthalpy (ΔH˚) and Entropy (ΔS˚) were evaluated using Fig.3.15 at all the temperatures and shown in Table 3.3. The negative values of ΔG˚ indicated that the adsorption process was spontaneous in nature with higher affinity of dye towards adsorbent surface. The positive value of ΔH˚ indicated that the process was endothermic and the positive value of ΔS˚ indicated increased randomness at adsorbent surface. The adsorption process was involved with a dissociative mechanism following the second law of thermodynamics.
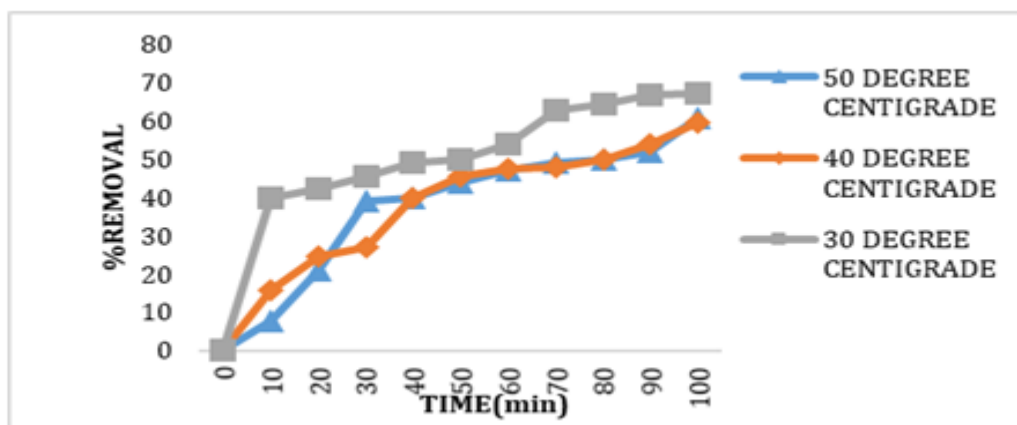
Fig. 3.15. Effect of temperature on %Removal MG
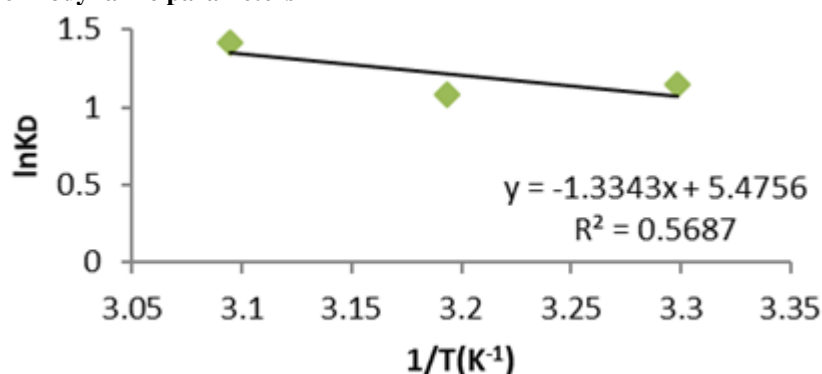
3.3.7 Plot for thermodynamic parameters

$$y = -1.3343x + 5.4756$$
$$R^2 = 0.5687$$

Fig.3.16. Adsorption kinetics

S.No	T(K)	K_d	ln K_d	ΔG°(KJ/mole)	ΔH°(KJ/mole)	ΔS°(KJ/mole)	E_a (J/mole)
1	303.15	3.1282	1.1404	-2.8742			
2	313.15	2.9382	1.0777	-2.8058	11.0933	45.524	0.0008
3	323.15	4.1255	1.4171	-3.8072			

Table 3.3: Adsorption Thermodynamics parameters of MG

3.3.8 Adsorption Kinetics

The adsorption kinetics of MG dye onto RHA was examined using batch studies. The kinetic parameters plays a key role in designing and modeling the rate process. Different kinetic models were suggested to find out the adsorption mechanism. The pseudo-first and pseudo-second order kinetics were plotted as shown in Fig 3.17 & 3.18 respectively. On comparison of R^2 values from Table 3.4, it was found that adsorption data of MG was better fitted in pseudo second order model and that the process of removal of MG using RHA as an adsorbent was second order kinetics.
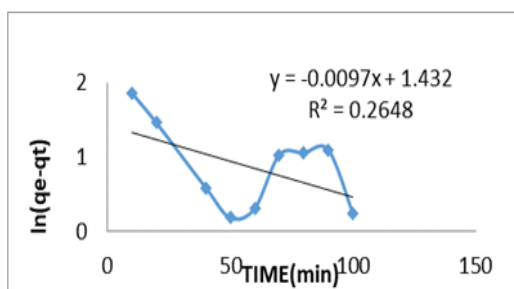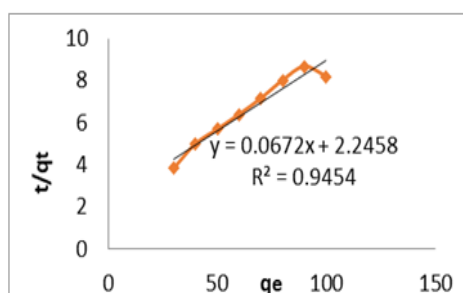

$$y = -0.0097x + 1.432$$
$$R^2 = 0.2648$$

Fig. 3.17. Pseudo-first order curve

$$y = 0.0672x + 2.2458$$
$$R^2 = 0.9454$$

Fig. 3.18. Pseudo-second order curve

Order	C_o (mg/L)	q_e, Exp (mg/g)	q_e, Cal (mg/g)	k_1(1/min)	R^2
Pseudo-first order	10	10.846	4.1870	0.0097	0.2468
Pseudo-second order	10	10.846	12.348	0.002010	0.9459

Table 3.4: Parameters of Pseudo-first and Pseudo-second order

3.3.9 Langmuir Isotherm:

This isotherm can be valid as a monolayer adsorption of solute on adsorbent surface having infinite number of identical active sites. It is based on the assumption that uniform energies of adsorption take place onto the surface of adsorbent without any migration in a surface plane. The intercept gives the q_o value and slope gives the b value as given in Table 3.5. The Langmuir isotherm was shown in Fig.3.19.
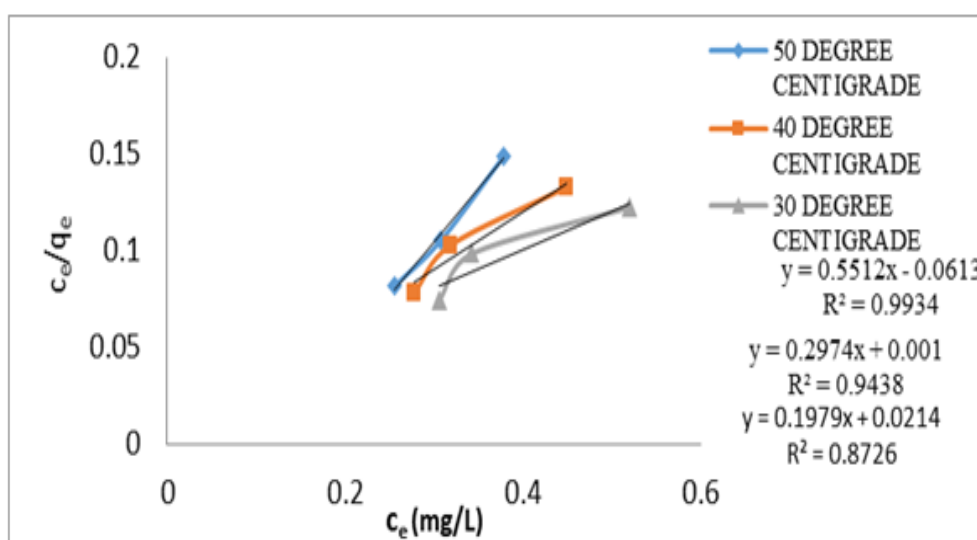

Fig.3.19. Langmuir isotherm curve

3.3.10. Freundlich Isotherm:

The Freundlich isotherm was shown in Fig.3.20, where q_e is the amount of MG dye adsorbed (mg/g), C_e is the equilibrium concentration of dye in solution (mg/L), and K_f and n are constants values shown in Table 3.5, including the affecting factors on adsorption intensity and capacity of adsorption.
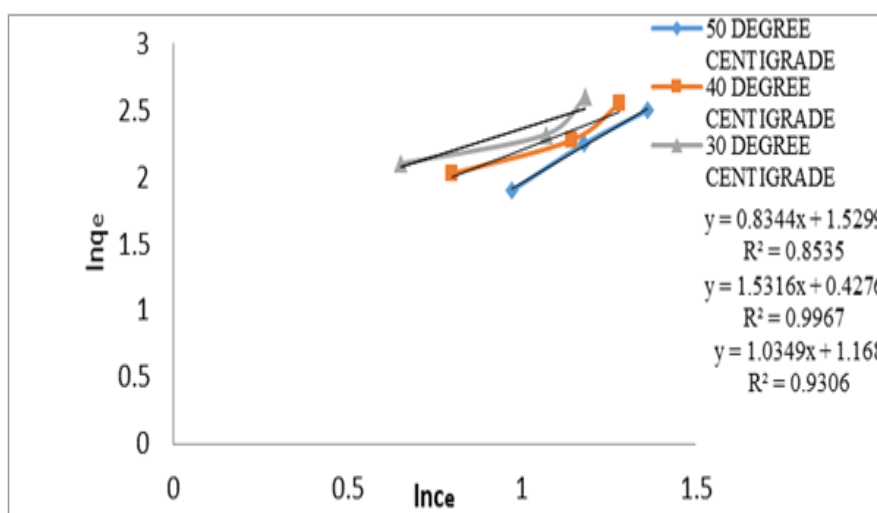

Fig.3.20. Freundlich isotherm curve

		Temperature 30˚C	Temperature 40˚C	Temperature 50˚C
Langmuir Isotherm	R^2	0.9934	0.9438	0.8726
	q_o	46.728	12.315	16.313
	b	0.1081	0.2730	0.1112
Freundlich Isotherm	R^2	0.9967	0.9306	0.8535
	n	2.3386	0.8561	0.653
	K_f	4.6255	2.8148	2.3034

Table 3.5: Adsorption Isotherms

IV.   CONCLUSION

Rice Husk Ash exhibited significant adsorption capacity for Malachite Green dye under suitable experimental conditions. The characterization studies with FTIR and SEM were proved the existence of significant pores and different functional groups on RHA, which were participated during adsorption process. The equilibrium was attained at an optimal contact time of 100 minutes. The optimum experimental values of effecting factors like initial dye concentration, adsorbent dosage, agitation speed and pH in this study were found to be **10 mg/L, 0.15 g, 100 and 8**, respectively. The correlation coefficient, R^2 value and corresponding to experimental q_e value was favored pseudo-second order kinetics and thus adsorption process was a pseudo-second order reaction with $k_1 = 0.002010$ and $R^2 = 0.9459$. The Freundlich adsorption model was fitted well since its R^2 value was higher that of Langmuir adsorption model. Thermodynamic parameters like change in Gibbs free energy ($\Delta G˚$), Enthalpy ($\Delta H˚$) and Entropy ($\Delta S˚$) were evaluated at all the temperatures. The negative values of $\Delta G˚$ indicated that the adsorption process was spontaneous in nature with higher affinity of dye towards adsorbent surface. The positive value of $\Delta H˚$ indicated that the process was endothermic and the positive value of $\Delta S˚$ indicated increased randomness at adsorbent surface. The adsorption process was involved with a dissociative mechanism following the second law of thermodynamics.

V.   REFERENCES

[1].   Yong Zhang et al, Journey of Chemistry, Volume 2017 and Article ID 1936829.
[2].   S. Nirmala et al, International Journal of Scientific and Research Publications, Volume 6, Issue 9, September 2016.
[3].   I.A. Rahman et al, School of Chemical Sciences, University Sains Malaysia, 11800 Penang, Malaysia.
[4].   S. A. Abo-El-Eneina et al, Journal of Hazardous Materials, Volume 172-2009, pages: 574-579.
[5].   Mohd Azmier Ahmed and Rasyidah Alrozi, Chemical Engineering Journal, Volume 71-2011, pages: 510-516.
[6].   Mi-Hwa Baek et al, Journal of Hazardous Materials 176(2010), pages: 820-828.
[7].   Shamik Chowdhury et al, Journal of Separation Science and Technology, Volume 46, Issue 12-2011.
[8].   Neeraj Jain et al, IOSR Journal of Environmental Science, Toxicology and Food Technology (IOSR –JESTFT), Volume 9, Issue 6 Ver. I (Jun. 2015), pages 42-50.
[9].   Vivek Ganvir and Kalyan Das, Journal of Hazardous Materials, Volume 185-2011, pages: 1287-1294.
[10].   K. Y. Foo and B. H. Hameed, Journal of Advances in Colloid and Interface Sciences, Volume 152-2009, pages 39-47.
[11].   V. M. Muinde et al, Journal of Environmental Protection, Issue 8-2017, pages: 215-230.
[12].   Binod Kumar and Upendra Kumar, Korean Journal Chemical Engineering, Volume 32, Issue 8-2015, pages: 1655-1666.
[13].   S. D. Khattria and M. K. Singh, Journal of Hazardous Materials, Volume 167-2009, pages: 1089-1094.
[14].   Venkat S. Mane et al, Journal of Environmental Management 84(2007), pages: 390-400.
[15].   Soumitra Banerjee et al, International Journal of Advanced Engineering and Science (IJAEMS), Volume 3, Issue 4-2017.
[16].   Ashish S. Sartape et al, Arabian Journal of Chemistry, Issue 10-2017.
[17].   Mamdouh S. Masoud et al, Arabian Journal of Chemistry, Issue 9-2016.
[18].   T. Santhia et al, Journal of Hazardous Materials, Volume 179-2010.
[19].   Wen-Tien Tsaia and Huei-Ru Chen, Journal of Hazardous Materials, Volume 175-2010.
[20].   Uma et al, Journal of Industrial and Engineering Chemistry, Volume 19-2013.
[21].   Anbia. M and A. Ghaffari, Journal of Iranian Chemical Society, Volume 8- 2011, pages: 67-76.
[22].   Chen. H and J. Zhao, Adsorption, Volume 15, Issue 4-2009, pages: 381-389.
[23].   Gowswami et al, International Journal of Scientific Research and Management (IJSRM)-2014, pages: 842-845.
[24].   Grabowska Ewa Lorenc and Gryglewicz Gra Zyna, Elsevier, Dyes and Pigments, Volume 74, Issue 1-2007, Pages: 34-40.
[25].   B. H. Hameed et al, Journal of Hazardous Materials, Volume 141-2007, Pages: 819-825.
[26].   Hameeda. B. H et al, Journal of Hazardous Materials, Volume 159-2010, pages: 574-579.
[27].   Indra Deo Mall et al, Colloids and Surfaces, Volume 264-2006, Pages: 17-28.
[28].   Oladoja. N. A. et al, Turkish Journal of Engineering and Environmental Sciences, Volume 32-2008, Pages: 303-312.
[29].   Uddin et al, ARPN Journal of Engineering and Applied Sciences (2006-2007).
[30].   Robert E. Trybal," MASS – TRANSFER OPERATIONS", Third Edition, McGraw – Hill International Editions (1981).
[31].   B K Datta, "Principles of Mass Transfer and Separation Processes", Prentice Hall of India Pvt Limited, New Delhi.
[32].   Christie J. Geankoplis, "Transport processes   and unit operations"